energies

Review

Review of the Heat Flow Mapping in Polish Sedimentary Basin across Different Tectonic Terrains

Jacek Majorowicz †

Department of Physics, University of Alberta, Edmonton, AB T6G 2R3, Canada; majorowi@ualberta.ca or majorowicz@shaw.ca
† Presently at Northern Geothermal Consult., 105 Carlson Close, Edmonton, AB T6R2J8, Canada.

Abstract: Heat flow patterns variability related to the age of the consolidated, and differences in, sedimentary thickness of the sedimentary succession are important constraints upon the thermal state of the sedimentary fill and its geothermal energy potential. Heat flow in the Permian basin of central Europe varies from a low of 40 mWm^{-2} in the Precambrian Platform to 80 mWm^{-2} in the Paleozoic basement platform influencing temperature for geothermal potential drilling depth. Continuity of thermal patterns and compatibility of heat flow Q across the Permian basin across the Polish–German basin was known from heat flow data ever since the first heat flow map of Europe in 1979. Both Polish and German heat flow determinations used lab-measured thermal conductivity on cores. This is not the case for the recent heat flow map of Poland published in 2009 widely referenced in Polish geological literature. Significant differences in heat flow magnitude exist between many historical heat flow maps of Poland over the 1970s–1990s and recent 21st century patterns. We find that the differences in heat flow values of some 20–30 mWm^{-2} in Western Poland exist between heat flow maps using thermal conductivity models using well log interpreted mineral and porosity content and assigned world averages of rock and fluid thermal conductivity versus those measured on cores. These differences in heat flow are discussed in the context of resulting mantle heat flow and the Lithosphere-Asthenosphere Boundary depth modelled differences and possible overestimates of deep thermal conditions for enhanced geothermal energy prospects in Poland.

Keywords: heat flow; LAB; central Europe basin; tectonic units

check for updates

Citation: Majorowicz, J. Review of the Heat Flow Mapping in Polish Sedimentary Basin across Different Tectonic Terrains. *Energies* **2021**, *14*, 6103. https://doi.org/10.3390/en14196103

Academic Editors: Carlo Roselli and Alexei V. Milkov

Received: 1 August 2021
Accepted: 6 September 2021
Published: 24 September 2021

1. Introduction

The knowledge of heat flow Q, (Q = λ*gradT, where λ is thermal conductivity and gradT is geothermal gradient of temperature T) is crucial for the prediction of deep geothermal resources below maximum depth of temperature logs and the estimate of geothermal energy potential of sedimentary basins and potential of the enhanced geothermal systems (EGS) [1–4]. The Central European transition from the Precambrian platform to younger tectonic basement Caledonian, Variscan, Alpine terrains shows significant differences in crustal structure, age (Figure 1a,b), [5,6] and magnitude of Q, especially evident in Poland where all these differing tectonic elements are present under sedimentary succession reaching as high as 13 km [7] in the axis of the Polish–German basin.

In this paper I review the evolution of Polish heat flow maps since the first ones of 1972–1973 by Majorowicz [8,9] through some four decades by many contributors [10–17]. All the heat flow data in Poland, except a few wells reaching crystalline rocks of Sudetes [10], come from wells into the sedimentary strata. I will focus on apparent differences in magnitude of some 20–30 mWm^{-2} between Polish heat flow maps. The context of such discrepancy in surface heat flow upon heat flow at the consolidated basement and mantle heat flow will be reviewed. The patterns of heat flow and depth level temperatures run across different age tectonic units/terrains and its relationship to these has been difficult to pinpoint [18]. The estimates of depth of LAB (Lithosphere-Asthenosphere Boundary) from the observed differing heat flow maps of Poland and seismological constraints on the LAB boundary will be reviewed and discussed.

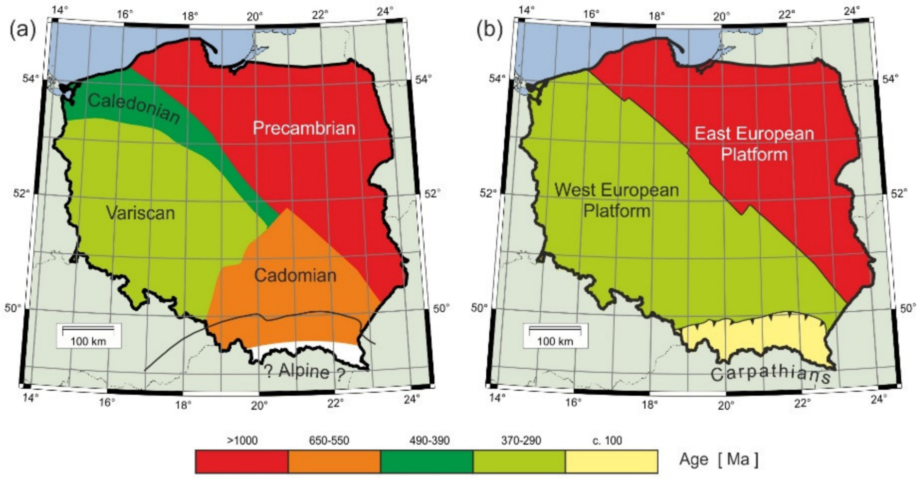

Figure 1. Newly drafted compilation of major division of the Poland area on tectonic mega-units according to (**a**) [6] and (**b**) [19]. Note: The original colors were modified to show both maps in the same common color pattern.

2. The Tectonic Background

Tectonic subdivision of the consolidated basement in Poland is shown in Figure 1a according to Karnkowski [20] and in Figure 1b according to Żelaźniewicz et al. [19]. The age of the basement is given, and it changes from less than 100 Ma for the Carpathian forefront zone to >1000 Ma for the Precambrian basement of the East European Platform as shown in Figure 1a,b. The Alpine zone of the Carpathian is an external zone of the Carpathians with an older basement beneath (Figure 1a,b).

Sedimentary fill in the Polish basins vary from just few hundred meters in Northeastern Poland and exposed crystalline rocks in Sudetes of southwestern Poland to some 15 km thickness in the Polish Trough in the central-northern Poland as based on 3D seismological modeling by Grad and Polkowski [7] from numerous seismic profiles cutting across sedimentary basins (Figure 2). The 3D geometry of the crust and upper mantle down to 60 km was studied before [7,21], and the creation of Moho depth which in Poland varies from 29 km in the Variscan southwestern Poland to 49 km in the Precambrian platform (Figure 2b).

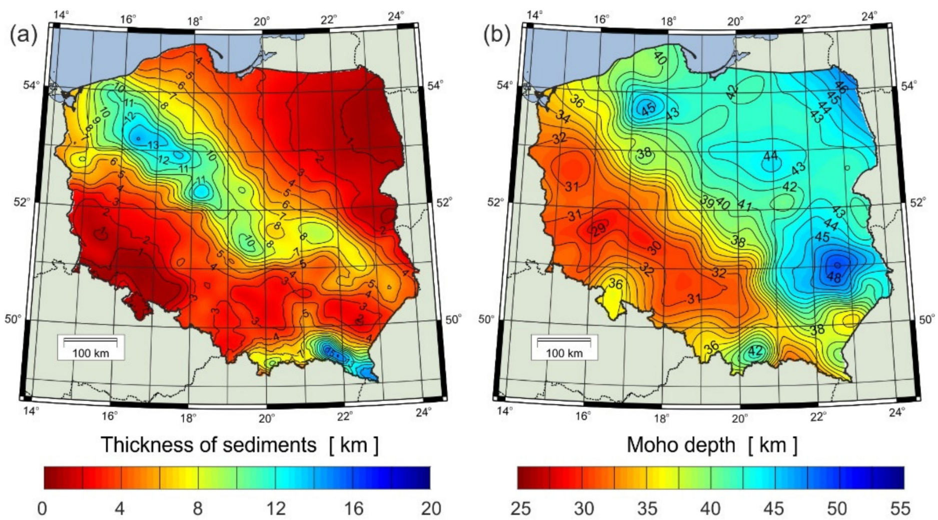

Figure 2. Thickness of sedimentary succession (**a**) and Moho depth (**b**) in Poland from Grad et al. [21], modified/redrafted.

3. Historical Evolution of Heat Flow Maps of Poland—Materials and Methods

We can observe significant differences existing between many historical heat flow maps of Poland published over the 1970s–1990s with no paleoclimatic correction applied and recent 21st-century maps for which Q data had paleoclimatic influence taken into corrections. Heat flow maps drawn from different density Q data and based on different approaches to its calculations show differences of some 20–30 mWm^{-2}. These are observed despite recent maps that considered paleoclimatic correction for glacial-interglacial surface forcing (Szewczyk and Gientka, [17], Majorowicz and Wybraniec [22]).

The terrestrial heat flow Q was calculated as a product of geothermal gradient grad T(z), where T is temperature at depth z and thermal conductivity for rocks λ in depth interval Δz for which grad T(z) was determined. Thermal conductivity λ at an interval Δz_i (number "*i*"of rock components) may be determined by:

(1) averaging the measurement made on core samples from the interval;
(2) using the mean values for stratigraphic lithologic layers calculated for a large territory by numerous borehole data;
(3) building a geophysical log-based model of the volume of number "*i*" of rock components with l *i*-thermal conductivity of mineral components from tables, *Vi*-volume of component "*i*" and porosity.

Method (1) was used to calculate λ for Q determinations for the first heat flow maps of Poland, by Majorowicz [9,23,24], based on N = 52 data. The same method was used by Plewa published in Majorowicz and Plewa [14], who made Q determinations in Poland and in the latest compilation listed N = 87 Q values.

Method (2) was used by Gordienko and Zavgorodnyaya [11]) who estimated Q for N = 176 data points and by Karwasiecka and Bruszewska [12] for N = 274 Q data used for heat flow maps of Poland. They were verifying the patterns by Q data from thermal equilibrium geothermal gradients and λ measured on cores.

Method (3) was used by Szewczyk and Gientka [17]) for N = 308 Q based heat flow map (unlisted data points).

The Q magnitude difference is observed between maps for Poland (Figures 3–5). These are based accordingly on Q calculations from return grad T(z) corrected for thermal equilibrium from deep well temperature profiles and measured averaged thermal conductivity λ from core samples by Majorowicz [9,23,24], Majorowicz and Plewa [14], and Karwasiecka and Bruszewska [12], versus Grad T(z) and thermal conductivity profiles build from models of rock content and porosity from geophysical well logs and assigned table averages of λ for these rocks by Szewczyk and Gientka [17].

High surface heat flow Q_0 = 65–80 mWm^{-2} is a regional feature characteristic for the South-Western part of Poland. This enlarged Q 'height' (Figure 5) occurs between the Middle Odra Horst to SW and the Variscan Deformation Front (Majorowicz and Wybraniec [22], Majorowicz and Šafanda [26], Puziewicz [16] and Figure 5 in this paper). Despite the differences in absolute values of some 20–30 mWm^{-2} due to differences in thermal conductivity models, estimated from well logs by Szewczyk and Gientka, [17] versus those measured on cores (Majorowicz and Plewa [14], Karwasiecka and Bruszewska [12], and Majorowicz and Wybraniec [22]), Q patterns are similar in several maps (Figures 3–5). However, analysis of this difference in Q between maps shows that heat flow values in Figure 4b of some 100 mWm^{-2} are likely overestimates. This will be discussed in further analysis.

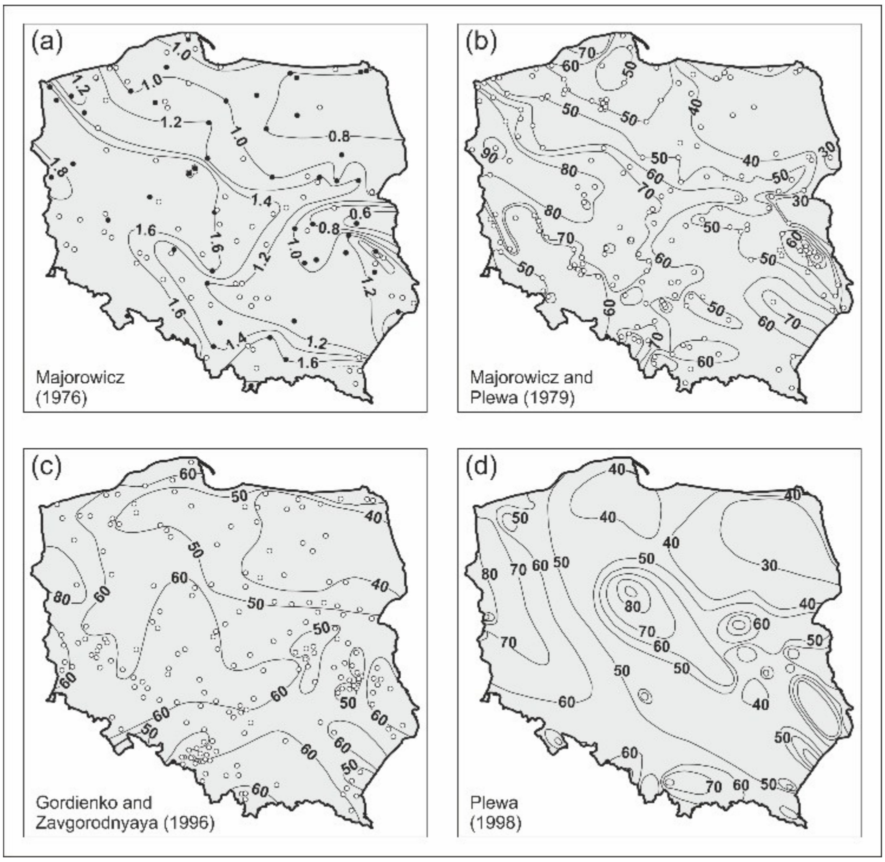

Figure 3. Historical heat flow maps of Poland according to different authors: (**a**) Majorowicz [24])–in this map Q values are in old heat flow units HFU (1 HFU = 10^{-6} cal/(cm^2 s) = 41.84 mWm^{-2}). (**b**) Majorowicz and Plewa [14]. (**c**) Gordienko and Zavgorodnyaya [11]). (**d**) Plewa [15]. For figures (**b**–**d**) heat flow values are in mWm^{-2}. (New figure).

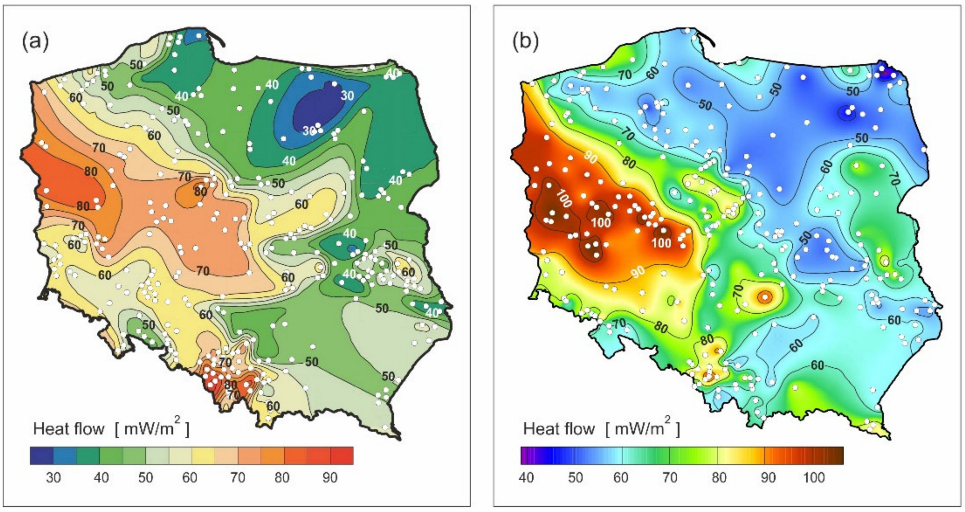

Figure 4. Heat flow maps of Poland according to Karwasiecka and Bruszewska [12]) (**a**) and Szewczyk and Gientka [17] (**b**). Note some 20–30 mWm^{-2} difference in average heat flow magnitudes between both maps. The original maps were redrafted and modified for common graphics (free software for mapping is from [25].

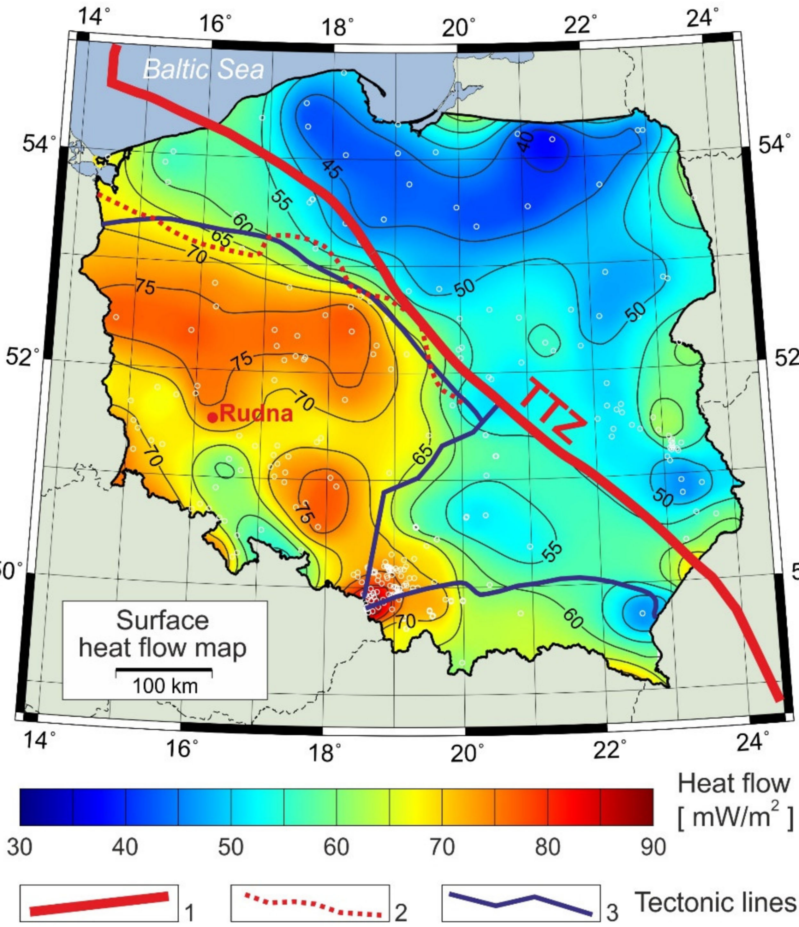

Figure 5. Surface heat flow map of Poland based on heat flow data corrected for paleoclimate according to Majorowicz and Wybraniec [22]. White circles show the distribution of boreholes with heat flow data. Big red dot shows location of the test site Rudna. Note some 20–30 mWm^{-2} difference in average heat flow magnitudes between this map and the map in Figure 4b.

Major tectonic lines like TTZ are not evident as exact boundaries between low Q east and west of it. Low heat flow at all depth levels like base of sediments and Moho extends west of TTZ. In general, it extends to the magnetic line depicting the southern margin of the Pomeranian Massif [27]. In the south-west of TTZ it extends partially into the Cadomian area in Southern Poland [14,28], Figure 5. The boundary depicting the reach of the Carpathian foreland (see Figure 2) is not showing as a Q boundary on any of the analyzed maps in Figures 3–5. Q low increases from the eastern part of the Cadomian basement beneath Northern Carpathians (compare Figures 2 and 5) and goes into Q high in the west across the E-W boundary of the Carpathian foreland zone.

Heat flow values shown in Figure 5 are well within the heat flow vs. tectonic age relation bounds (Figure 6). On the other hand, heat flow values range from the Szewczyk and Gientka [17] map redrafted in Figure 4b are well above these bounds. It is an especially strong discrepancy for the Variscan age area. This observation will be explored farther down in the Discussion section.

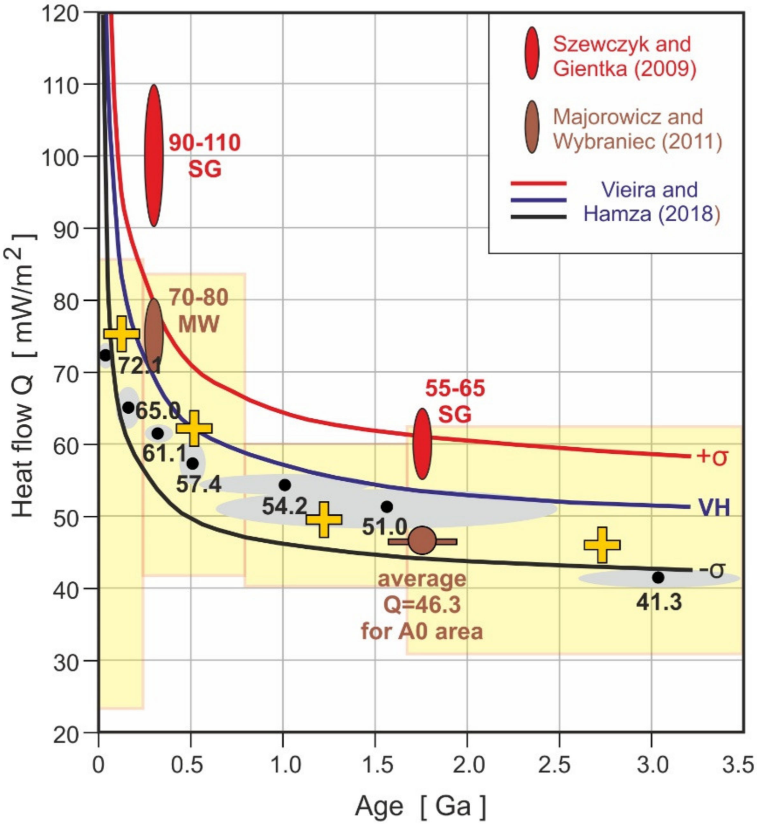

Figure 6. Comparison of average values of the continental heat flow Q for tectonic units of different age. Averaged values, for "13 BB Star" array in northern Poland (marked A0) is shown by big brown dot with line of age range. Average heat flow-age groups from Szewczyk and Gientka [17] marked SG (red ellipses), and Majorowicz and Wybraniec [22] marked MW (brown ellipses), differs significantly. MW data fit the expected heat flow versus age relationship much better. Heat flow-age compiled from Jessop et al. [29] and Majorowicz and Jessop [14] are shown by yellow crosses with the range shown yellow areas. Heat flow vs. age relationship lines marked by VH and the standard deviation bounds (_+σ and −σ) are from Vieira and Hamza [30].

4. Heat Flow at the Base of Sediments (at the Consolidated Basement) and at the Moho

Heat flow at the base of compacted sediments (see [31,32] for the effect of compaction and consolidation of sedimentary fill upon sedimentary thermal state) and at the Moho (mantle [33] contribution below the crustal part) were calculated by Majorowicz et al. [18] using the down-stripping method [34–37] for the heat generation parts of heat flow contribution of the sediments and crustal heat generation heat flow contribution. These can be compared respectively in Figures 7 and 8 below.

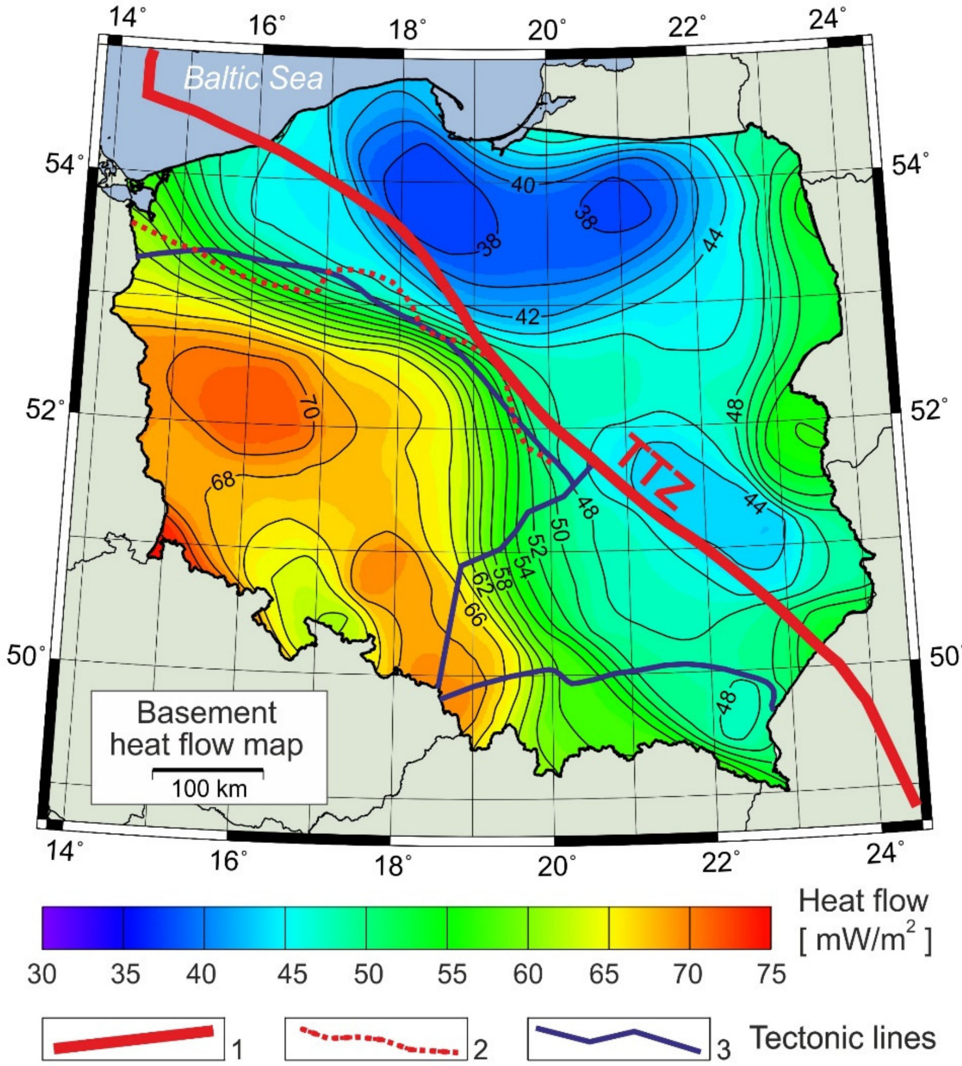

Figure 7. Newly drafted base of sediments level heat flow map of Poland. Tectonic lines: 1—position of the TTZ in Poland according to Narkiewicz et al. [38], 2—magnetic line, southern margin of the Pomeranian Massif is after Królikowski [27], 3—basement borders after Karnkowski [6].

The sedimentary rocks contribute significant radiogenic heat production and Q_0 at the surface minus Q contribution of sedimentary cover is up to 20 mWm^{-2} with the largest reduction of Q just west of TTZ in the Mid-Polish Swell, where the thickness of sedimentary cover is >10 km (Figure 2). The comparison of the above Q maps at the base of sedimentary fill and at the base of the crust at Moho (Figure 7 vs. Figure 8) shows that general patterns (trends in heat flow) are similar. However, a large difference in magnitude of Q exists due to a contribution of the radiogenic heat generation of the upper crystalline crustal rocks. Crustal and mantle heat flow contributions studied elsewhere [20,37,39–42] point to large un-certainty in calculations of crustal vs. mantle heat flow contributions with estimates 40% vs. 60% of total surface heat flow [20,37,39].

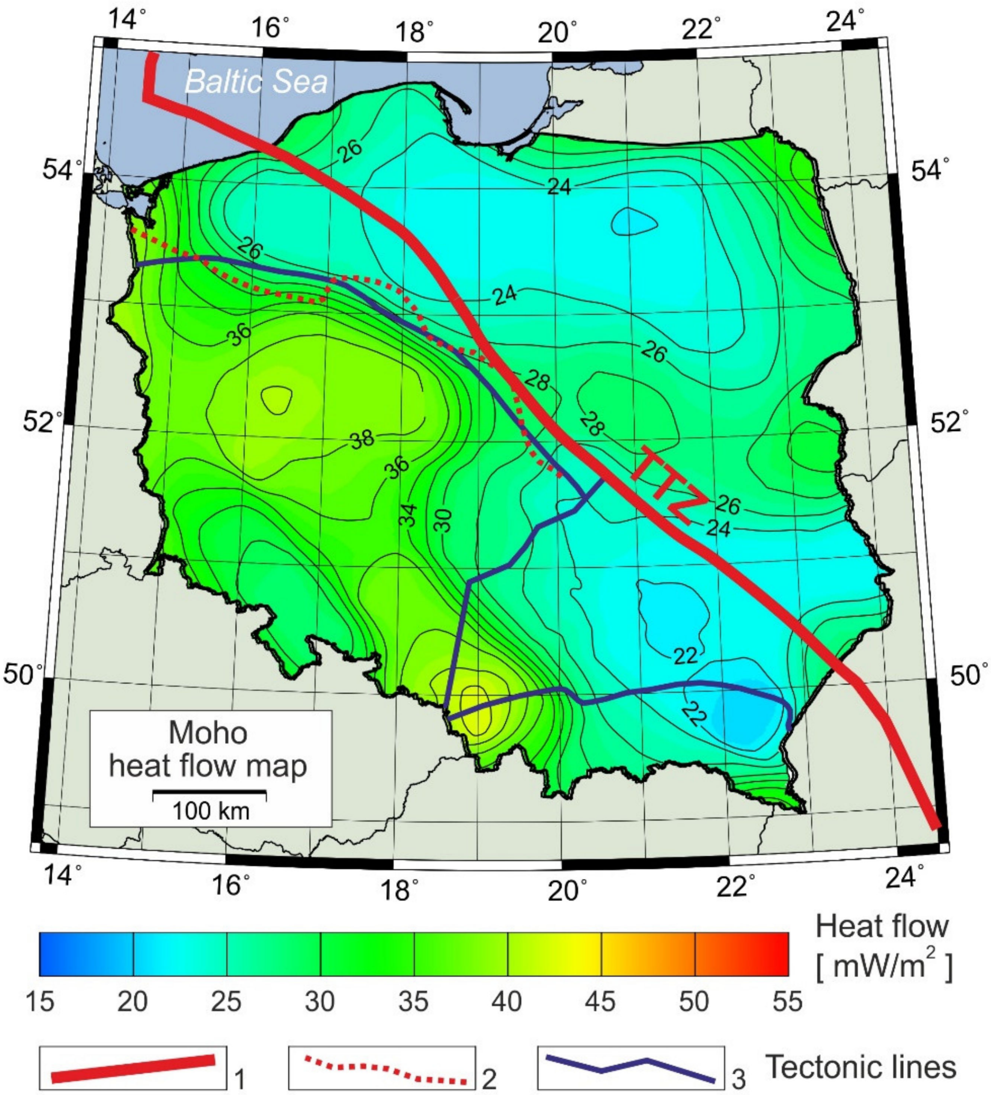

Figure 8. Moho heat flow map of Poland (redrafted and color scale modified from Majorowicz et al., 2019, [18]. Tectonic lines: 1—position of the TTZ in Poland according Narkiewicz [38], 2—magnetic line, southern margin of the Pomeranian Massif after Królikowski [27], 3—basement borders after Karnkowski (2008, [6]).

5. Polish Heat Flow in the European Map Context

The Q map for paleoclimate heat flow of the European continent was corrected by Majorowicz and Wybraniec [22], and Figure 9 used heat flow data corrected for the paleoclimatic effect.

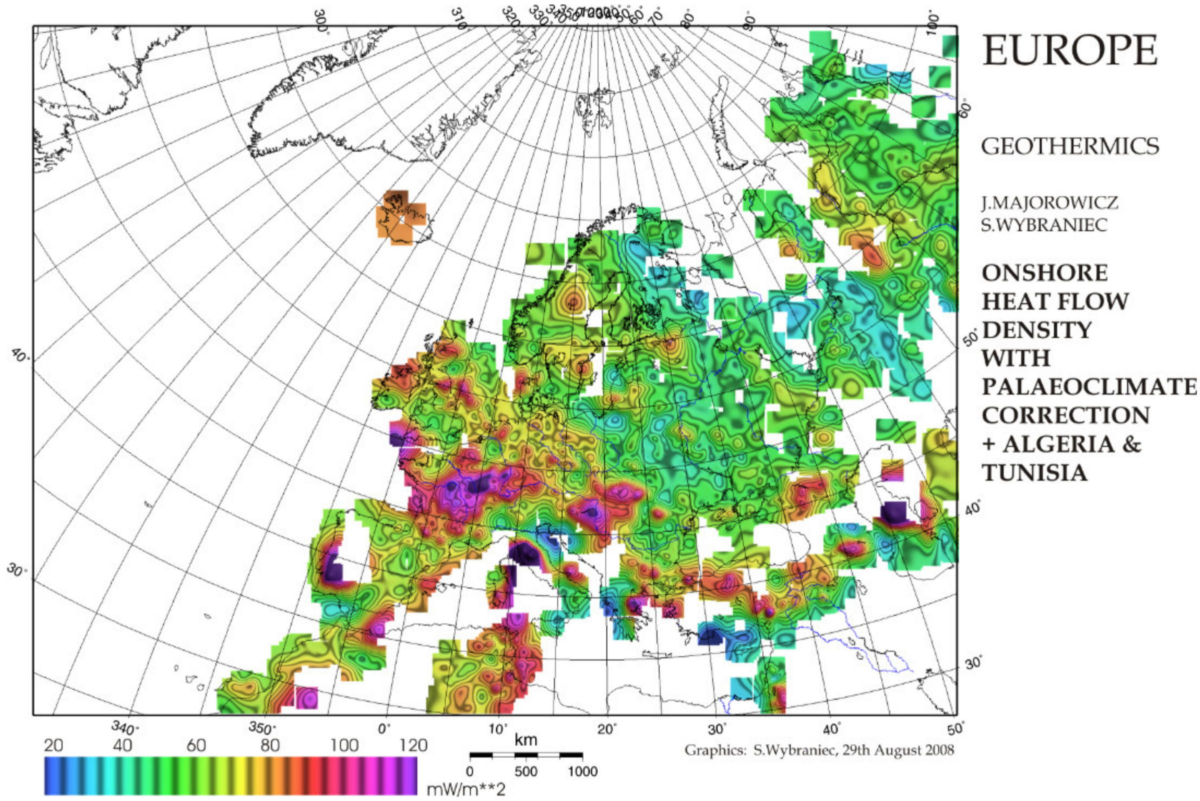

Figure 9. Heat flow map of Europe based on forcing heat flow values corrected for glacial-postglacial (Majorowicz and Wybraniec, redrafted unpublished version). Q data used later in a published paper by Majorowicz and Wybraniec [22] are available upon request as an Excel file.

The previous heat flow maps in the Geothermal Atlas of Europe (Čermak and Hurtig [43,44], Q map of Cloething et al. [45] and Q map of Hurtig et al. [46], had no paleoclimatic correction applied.

The Q map of Europe by Majorowicz and Wybraniec [22] shows the context of Polish heat flow transition between Precambrian and Paleozoic Platforms. The Central European heat flow map (Figure 10) compiling Polish and neighboring heat flow data from heat flow map of Europe of Majorowicz and Wybraniec [22] and of the European Permian basin Q map by Guterch et al. [47] show that the Q transition between the Polish and German basins is continuous in the patterns and magnitude across the German–Polish border in the northern German–Polish Basin (GPB). This is also true for the data used in Figure 10 map based on Majorowicz and Wybraniec [22] data corrected for glacial–postglacial surface temperature change forcing paleoclimatic correction [13,22,26] (data upon request).

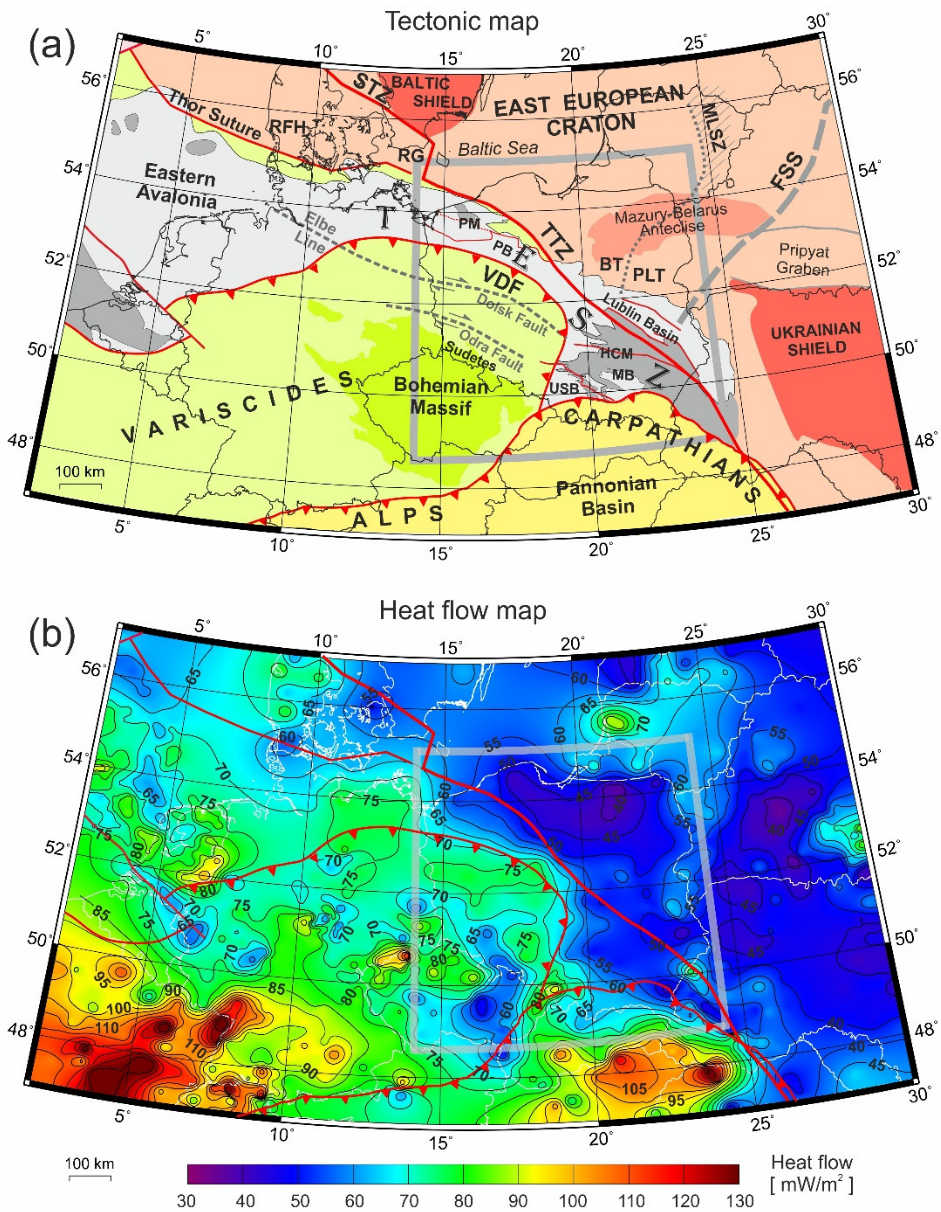

Figure 10. Tectonics and heat flow. (**a**) Tectonic sketch of the pre-Permian Central Europe in the contact of the East European Craton, Variscan and Alpine orogens compiled by Grad et al., 2016 [7,48] and Narkiewicz et al. (2011 [38]) is redrafted/modified from Majorowicz et al. [18]. BT-Baltic Terrane; FSS—Fennoscandia-Sarmatia Suture; HCM—Holy Cross Mountains; MB—Małopolska Block; MLSZ—Mid-Lithuanian Suture Zone; NEGB—North-Eastern German Basin; PB—Polish Basin; PM—Pomerania Massif; RG—Rønne Graben; RFH—Ringkøbing-Fyn High; STZ—Sorgenfrei-Tornquist Zone; TESZ—Trans-European Suture Zone; TTZ—Teisseyre-Tornquist Zone; USB—Upper Silesian Block; VDF—Variscan Deformation Front. (**b**) Central European heat flow map based on corrected for paleoclimate heat flow data from Majorowicz and Wybraniec [22] with main tectonic lines. Grey frames show the location of the study area.

In the neighboring Poland Danish and North German Basin NGB, Fuchs [48] and Norden et al. [49] explore Q values for several km deep wells in the German basin west of the Polish study area for which heat flow was estimated for wells deeper than 1.5 km. Deeper than 1.5 km heat flow is less influenced by the glacial interglacial [50] surface temperature cycle. The influence at such depth will be close to or less than the error on Q from temperature T with depth z, grad T(z) and thermal conductivity λ errors towards Q determination. The surface temperature forcing signal due to glacial-postglacial history [50] is diffused with depth to the point that the magnitude of the Q paleoclimatic correction is <5 mWm^{-2} in the German—Polish Basin shown by Majorowicz and Šafanda [13], Majorowicz and Wybraniec [22] and Majorowicz and Majorowicz and Safanda 2018 [26]. In Central Europe, heat flow is significantly higher west of the Trans-European suture zone (TESZ) than for the East European Precambrian craton. High surface heat flow values >70 mWm^{-2} in Majorowicz et al., [18] and locally reaching up to 90 mWm^{-2} in Majorowicz and Šafanda [26] are the regional feature characteristic for the Western and South-Western Paleozoic Platform south-west of TESZ (see Figure 10a,b). This elevated Q and temperatures at different depth levels mainly occurs between the Odra Fault to South-West and the Variscan Deformation Front to the North-East (see this paper Figures 10b, 11, 12 and 13 in Szewczyk and Gientka [17], Figure 1 in Majorowicz and Wybraniec [22] and Figure 2 in Majorowicz and Šafanda [26]). This pattern stands out in all the published Q maps of the area of Central Europe despite the differences in absolute Q values described before, mainly due to differences in thermal conductivity λ models applied and assumed by various authors. These are estimated from composition of rock from the standard set of geophysical well logs and assumed from tables averages of λ for the components (Szewczyk and Gientka [17]) versus measured λ on cores (by Majorowicz and Plewa [14], Majorowicz and Wybraniec [22]). This elevated Q zone (Figure 1b) continues to the North-Eastern part of the German Basin, where average Q = 77 ± 3 mWm^{-2} and it reaches up to 91 mWm^{-2} for the 68–91 mWm^{-2} range (Norden et al. [49]. See also Figure 2 in Cloetingh et al. [45].) In southern Poland, heat flow increases from the modest values in the foreland zone of the Polish Carpathians (Wroblewska and Majorowicz [51]) to much higher values in the internal Carpathians, with the highest values in the Pannonian basin (Figure 10b), Simonova et al. [52,53]. High Q in the Miocene Pannonian basin (90 mWm^{-2} average) is locally >110 mWm^{-2} (Figure 10a). It was shown that locally heat flow can reach above 400 mWm^{-2} in active areas of Larderello and Monte Amiata in Tuscany, Italy but the background heat flow in the surrounding areas is quite normal and 70 mWm^{-2} according to Bellani [54].

6. Discussion

The observed 20–30 mWm^{-2} difference between heat flow maps of Poland and Germany is obvious from the compilation of the Szewczyk and Gientka [17] Q map and German Q data by Szuman et al. [55]. I highlighted the unbelievable 'jump' in values across the political Poland—Germany border in Figure 11 (this paper). There are several arguments discussed below for the possible reason for this likely overestimate in (Szewczyk and Gietka [17]) Polish data.

Heat flow maps of Poland (Figures 3–5) commonly show an increase in Q from low Q Precambrian-Cadomian and Caledonian terranes (Figure 5) to higher by some 20–30 mWm^{-2} Q in the Variscan basement platform area. The Variscan orogen of Europe characterized by the elevated Q was subjected to rifting and volcanism later. There, the latest volcanic Cenozoic lavas were locally migrating from the asthenosphere between 30 and 18 Ma at the T = 1400 °C (asthenospheric basanite solidus), [16,56]). Three-dimensional modelling [16] shows that it will explain only a relatively small (<4 mWm^{-2}) increase of the current Moho and surface heat flow. Glacial-interglacial extent variability [57] will not explain variability in deep >2km heat flow values. We cannot exclude that the Moho heat flow calculated in [16] and here (Figure 8), which indicates "warm" lithospheric mantle, can be an artefact, resulting from underestimation of radiogenic heat generation in the crust A as we do not consider the volume of rhyolites/granites related to the Permian igneous province which is not known. Q in the Polish Carpathian foreland has low to moderate values representing older basement units beneath thrust over-folded sedimentary succession. It increases towards the inner Carpathians and Pannonian basin.

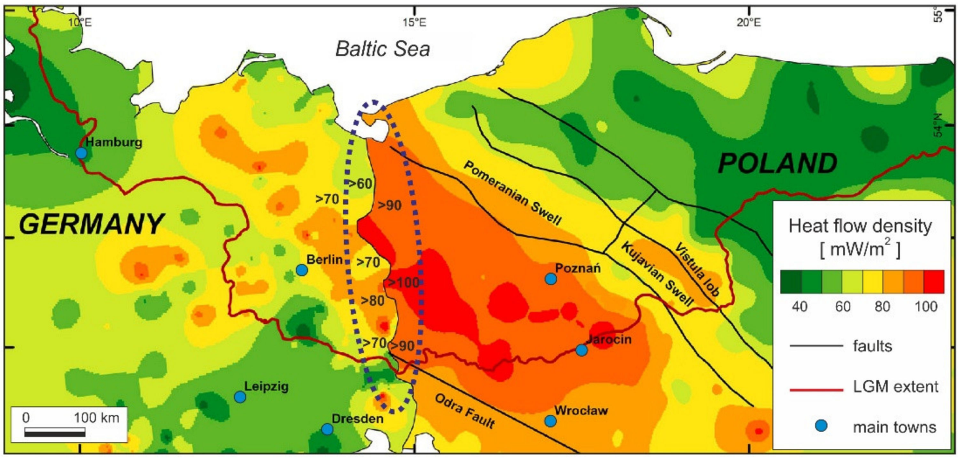

Figure 11. Compilation of heat flow map across the Germany–Poland border (modified and redrafted, based on Szuman et al., [55] data compilation from Global Heat Flow database for Germany data and heat flow for Poland from Szewczyk and Gientka [17]). Dotted blue line ellipse highlights the sharp jump of Q values at the border of Poland and Germany observed and highlighted here in this paper and this figure. The LGM red line shows the southern extent of the last glacial maximum at about 20–24 ka BP [50]. Note: the highlighted heat flow 'jump' at the political border is highly improbable.

The apparent jump in heat flow across the Polish–German political border (Figure 11) is in contrast with continuity of heat flow patterns in the Polish–German Basin when Majorowicz and Wybraniec [22]) heat flow data are used as shown in Figure 10b. This is also in contrast with what is known already from temperature at depth levels patterns ever since the Majorowicz [9]) temperature map at 1 km depth level for and Eastern Germany (Schloser [58]) shown here in Figure 12 according to [9]. These and deeper level temperatures (Figure 13a–c) are well withing the values suituable for geothermal energy use [59]. Recent deep temperature maps of Germany (Agemar et al. 0 [59]) show that the Northern German Basin has high temperatures >150 °C in parts of that basin at 4 km depth (see their Figure 3). A smooth transition of temperature patterns at 1 km, 2 km, 3 km depth levels (this paper Figures 12 and 13) is evident in the GPB basin with continuous geological-lithological transition between the border between Poland and Germany. It is apparent that it exists when temperature at depths of 1 km, 2 km and 3 km are compared (Figure 13a–c) in all three maps. A smooth transition of temperature patterns at 1 km, 2 km, 3 km depth levels is evident in the GPB basin with continuous geological-lithological transition between the border between Poland and Germany and it supports a smooth heat flow transition as in Figure 10b for the Variscan area.

It is impossible to have such continuity of temperature patterns across the German–Polish border and at the same area an obvious 'jump' in heat flow as shown in Figure 11 for the case of use of Szewczyk and Gientka [17]) heat flow data for Poland. There is no geological evidence of that "jump" relating to the thermal conductivity 'jump" to be needed for such a heat flow contrast. It would not make geological sense.

The German Q data 60–90 mWm^{-2} range are at the level of heat flow values in the basin east of the German Polish border as in recent Polish heat flow maps [18], also seen in heat flow maps in Figures 10b and 6 in this work. They are not in the range of Szewczyk and Gientka [17] heat flow map (Figure 4b) values 90–110 mWm^{-2} just east of the border with Germany (Figure 10). The most recent study in Templin deep well just northwest of the Polish-German border in the German basin shows Q = 58–69 mWm^{-2} for depth intervals within 1400–1600 m [33]. This depth is below the major influence of paleoclimatic forcing due to glacial/interglacial history, [13,22,33].

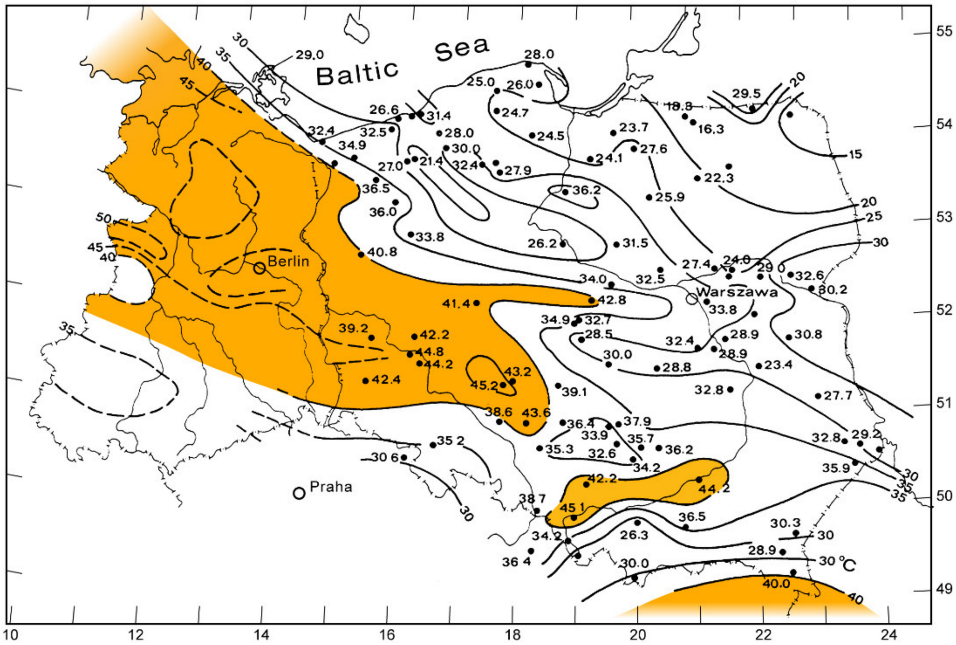

Figure 12. First temperature at 1 km map based Polish and Eastern Germany data redrafted and modified from Majorowicz 1973a, [9].

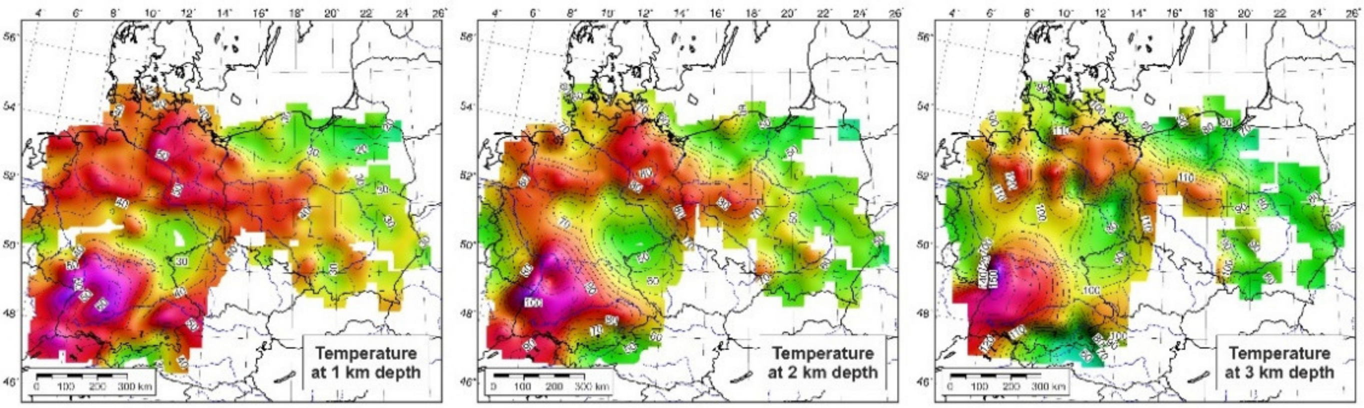

(**a**) (**b**) (**c**)

Figure 13. Compilation of temperature at depth (**a**) 1 km, (**b**) 2 km and (**c**) 3 km depth maps.

The difference of some 20–30 mWm^{-2} existing between the Q map of Poland exposed in this paper is not to be ignored. We need an explanation for such differences.

Heat flow continuity between German and Polish basins is observed from the Q maps of Europe by Majorowicz and Wybraniec [22]) and in Central Europe (Majorowicz et al. [18] and Figure 10b). Such continuity is not the case for the Q map compiled by Szuman et al. [55] for which the Szewczyk and Gientka [17] heat flow map was used.

We suspect, and more evidence is due from further research, that the differences in Q observed and described above are mainly due to differences in thermal conductivity models used for Q calculations. These are those estimated from well logs and world averages of rock thermal conductivities (Szewczyk and Gientka [17]) versus measured on cores. Significant differences exist between many historical heat flow maps of Poland over the 1970s, 1980s and recent 21st-century general patterns as to the above causes.

Q maps for which λ was a lab measure used by Karwasiecka and Bruszewska [12], (Figure 4a) and Majorowicz and Wybraniec [22], (Figures 5, 9 and 10b) show differences with the Q map for which geophysical well log-based λ estimates were used (Szewczyk and Gientka, [17] and Figure 4b). The latter are using mineralogical component of rocks and their porosity with table-based world averages of thermal conductivity λ of these components like in Table 4.3 in Barker [60]; Griffiths and Brereton [61]. Such a difference is apparent when comparing mean measured thermal conductivity for deep Polish basin sediments on cores. We have mean $\lambda = 2.3 \pm 0.4$ $Wm^{-1}K^{-1}$ for Polish basin wells listed by Majorowicz and Plewa [14] (their Tables 1–3) versus a well logs mean of $\lambda = 2.85 \pm 1$ $Wm^{-1}K^{-1}$ estimated from geophysical data in Szewczyk and Gientka [1], their Figure 5c. Such a difference in λ will easily explains difference in Q as high as 20 mWm^{-2} between Q maps from the two methods used. In western Poland grad T(z) = 35 mKm^{-1}. In such a case, for $\lambda_1 = 2.3 \pm 0.4$ $Wm^{-1}K^{-1}$ $Q_1 = 80$ mWm^{-2} and for $\lambda_2 = 2.85 \pm 1$ $Wm^{-1}K^{-1}$ $Q_2 = 100$ mWm^{-2}; 20 mWm^{-2}. The suspected reason for this difference is poor calibration of well-log-based λ estimates data due to poorly assumed literature tables of average l components of rocks. These usually change in a large range (Blackwell and Steele [62]; Blackwell and Richards [63] and Fuchs [48]). Such models work but need to be properly validated by TC laboratory data.

A large part of sedimentary clastics in the GPB are shales or sedimentary rocks with large shale content. $\lambda = 1.4$ $Wm^{-1}K^{-1}$ assumed by Szewczyk and Gientka [17] is some 0.3 $Wm^{-1}K^{-1}$ higher than some of the measured cores as evident from their Figure 5a,b. Thermal conductivity of shales or shaly sedimentary rocks analyzed by in situ experiments in deep wells for which precise in situ measurements combined with lab measurements compared by SMU David Blackwell lab [62–64] show that λ for shales can be closer to 1 W $m^{-1}K^{-1}$, e.g., which is some 0.4 $Wm^{-1}K^{-1}$ less than assumed in [17] for their well log derived component of sediments. While Blackwell and Steele [62–64] data are on shales from American basins, these may shed some light on overestimation of those assumed from world data-based tables. In fact, Polish data analysis shows that in numerous cases estimates of thermal conductivity from poorly calibrated well logs in [17] are higher than measured conductivity values on rocks for the same well examples [51].

It is apparent from our modelling (Figure 8), that the assumption of the high Q = 100 mWm^{-2} as a typical value for the western Poland after Szewczyk and Gientka [17]), (also in Szuman et al. [55]) versus lower Q = 70–80 mWm^{-2} after Majorowicz and Wybraniec and Majorowicz and Šafanda [22,26] would result in different Q at Moho, 55 mWm^{-2} vs. 35 mWm^{-2}, respectively. Such high Moho heat flow of 55 mWm^{-2} does not fit a general worldwide study and fits much younger tectonically active areas [37]. Some 40–50% of Q is from radiogenic heat in the crust and 50–60% comes from deeper sources in continental settings. Pollack and Chapman [37], Artemieva, [39] and Artemieva and Mooney [20]. Epelbaum et al. [41] suggest mantle heat flow is in the order of 15–84% of total.

The difference in surface heat flow between 80 and 100 mWm^{-2} also results in a calculated difference in the thermal LAB depth by some 42 km (Majorowicz et al. [18]). Values of mantle heat flow Q = 55 mWm^{-2} would be based on higher surface Q = 100 mWm^{-2} are "extremely" improbable (see Čermak, 1993, [34]; Majorowicz et al. [18]) and fit a much younger thin lithosphere like the Pannonian basin and not an old Variscan platform in south-western/western Poland. Puziewicz et al. [16]) who modelled input from Cenozoic alkaline volcanism at approximately 30–18 Ma in the South-western Polish platform showed that Q_M is in some 28–36 mWm^{-2} range which agrees with our Q_M = 26–38 mWm^{-2} range (see Figure 8). It locally may have been increased due to localized alkaline volcanic rock. It increased slightly the presently observed Q_0 and Q_M by approximately 4 mWm^{-2} only. We see much lower LAB depth (56 km) assuming Q = 100 mWm^{-2} for SW Poland from Figure 4b than assuming Q = 80 mWm^{-2} as in Figure 5 for the same site (LAB depth = 98 km). The depth of LAB = 98 km based on lower by 20 Q value is close, within 10 km, to the seismologically determined LAB (Wilde-Piórko et al. [65]). Recent mapping of LAB depth from several seismological and thermal data shows that depth 90–100 km is typical for much larger areas of southwestern Poland [18] and agrees with seismological LAB determinations.

7. Conclusions

Analysis of the difference between heat flow maps shown in this paper by several historical works leads to the conclusion that heat flow calculated from poorly calibrated thermal conductivity models from well logs [17]) and used in [55] for Poland are likely overestimates. Heat flow values as shown for the Variscan basement of Western Poland of some 100 mWm^{-2} and more in [17] are equal or higher than heat flow in the much younger tectonic areas in Europe like the internal Carpathians in the extensional zone of the Pannonian basin (Figures 9 and 10b). Heat flow in the Pannonian basin is 90–100 mWm^{-2} and locally reaches >110 mWm^{-2} (Figure 10b). There are evident geological and tectonic differences in the area between the young inner Carpathians [52,53]) and old Variscan basement Paleozoic Platform in Poland [16]. These tectonic and structural differences make it quite improbable for the heat flow to be the same between old Paleozoic Platform in southwestern Poland and the young Pannonian basin in Hungary [52,53].

The overestimated heat flow values in old platforms of Poland [17] need to be rejected in deep geothermal energy prospect analysis. The overestimated heat flow [17] will lead to overestimation of thermal conditions of deep basin below temperature log data in the zones where there is no deep well's control on in situ temperature. These are of interest for the future deep EGS geothermal electrical power prospects in deep Polish basins.

Funding: This research received no external funding.

Institutional Review Board Statement: Not applicable.

Informed Consent Statement: Informed consent was obtained from all subjects involved in the study.

Data Availability Statement: Data sets analyzed during the study be available upon request.

Acknowledgments: I acknowledge my deceased friends Stanislas Wybraniec and Mark Grad (Professor) on the studies we published together over the years and help with earlier published papers leading to this review. These are referenced in this review paper. Many thanks are due to two anonymous reviewers for their helpful comments.

Conflicts of Interest: The author declares no conflict of interest.

References

1. Blackwell, D.D. *Geothermal Resource Base Assessment the Future of Geothermal Energy: Impact of Enhanced Geothermal Systems (EGS) on the United States in the 21st Century*; Tester, J.W., Ed.; MIT Press: Cambridge, MA, USA, 2006.
2. Rybach, L. The Future of Geothermal Energy and its Challenges. In Proceedings of the World Geothermal Congress 2010, Bali, Indonesia, 25–29 April 2010.
3. Tester, J.W.; Reber, T.; Beckers, K.; Lukawski, M.; Camp, E.; Andrea, G.; Aguirre, A.; Jordan, T.; Horowitz, F. Integrating Geothermal Energy Use into Re-building American Infrastructure. In Proceedings of the World Geothermal Congress 2015, Melbourne, Australia, 19–25 April 2015.
4. Younger, P.L. Geothermal Energy: Delivering on the Global Potential. *Energies* **2015**, *8*, 11737–11754. [CrossRef]
5. Guterch, A.; Grad, M.; Keller, R.; Polonaise Working Group. Huge contrasts of the lithospheric structure revealed by new generation seismic experiments in Central Europe. *Prz. Geol.* **2004**, *52*, 753–760.
6. Karnkowski, P.H. Tectonic subdivision of Poland: Polish lowlands. *Prz. Geol.* **2008**, *56*, 895–903, (In Polish with English abstract).
7. Grad, M.; Polkowski, M. Seismic basement in Poland. *Acta Diabetol.* **2015**, *105*, 1199–1214. [CrossRef]
8. Majorowicz, J. Terrestrial heat-flow and geothermal gradient in north-east Poland. *Acta Geophys. Pol.* **1972**, *20*, 131–141.
9. Majorowicz, J. Heat flow in Poland and its relation to the geological structure. *Geothermics* **1973**, *2*, 24–28. [CrossRef]
10. Dowgiałło, J. The Sudetic geothermal region of Poland. *Geothermics* **2002**, *31*, 343–359. [CrossRef]
11. Gordienko, V.V.; Zavgorodnyaya, O.V. Estimation of heat flow in Poland. *Acta Geophys. Pol.* **1996**, *44*, 173–181.
12. Karwasiecka, A.M.; Bruszewska, B. Density of the surface Earth's heat flow on the area of Poland (Gęstość poerzchniowego strumienia cieplnego ziemi na obszarze Polski). *Centr. Arch. PIG Pol. Geol. Inst.* **1997**, *60*, 21–98. (In Polish)
13. Majorowicz, J.; Šafanda, J.; Torun-1 Working Group. Heat flow variation with depth in Poland: Evidence from equilibrium temperature logs in 2.9-km-deep well Torun-1. *Int. J. Earth Sci.* **2008**, *97*, 307–315. [CrossRef]

14. Majorowicz, J.; Plewa, S. Study of heat flow in Poland with special regards to tectonophysical problems. In *Terrestrial Heat Flow in Europe*; Čermak, V., Rybach, L., Eds.; Springer: Berlin/Heidelberg, Germany; New York, NY, USA, 1979; pp. 240–252.
15. Plewa, S. *Rozkład Parametrów Geotermalnych na Obszarze Polski*; Wydawnictwo CPPGSMiE PAN: Kraków, Poland, 1998; 138p.
16. Puziewicz, J.; Czechowski, L.; Grad, M.; Majorowicz, J.; Pietranik, A.; Šafanda, J. Crustal lithology vs. thermal state and Moho heat flow across the NE part of the European Variscan orogen: A case study from SW Poland. *Acta Diabetol.* **2019**, *108*, 673–692. [CrossRef]
17. Szewczyk, J.; Gientka, D. Terrestrial heat flow density in Poland—A new approach. *Geol. Q.* **2009**, *53*, 125–140.
18. Majorowicz, J.; Polkowski, M.; Grad, M. Thermal properties of the crust and the lithosphere–asthenosphere boundary in the area of Poland from the heat flow variability and seismic data. *Int. J. Earth Sci.* **2019**, *108*, 649–672. [CrossRef]
19. Żelaźniewicz, A.; Aleksandrowski, P.; Buła, Z.; Karnkowski, P.H.; Konon, A.; Oszczypko, N.; Ślączka, A.; Żaba, J.; Żytko, K. *Tectonic Subdivision of Poland*; KNG PAN: Wrocław, Poland, 2011; pp. 1–60. (In Polish)
20. Artemieva, I.; Mooney, W.D. Thermal thickness and evolution of Precambrian lithosphere: A global study. *J. Geophys. Res. Space Phys.* **2001**, *106*, 16387–16414. [CrossRef]
21. Grad, M.; Polkowski, M.; Ostaficzuk, S.R. High-resolution 3D seismic model of the crustal and uppermost mantle structure in Poland. *Tectonophysics* **2016**, *666*, 188–210. [CrossRef]
22. Majorowicz, J.; Wybraniec, S. New terrestrial heat flow map of Europe after regional paleoclimatic correction application. *Acta Diabetol.* **2010**, *100*, 881–887. [CrossRef]
23. Majorowicz, J.A. Heat Flow Data from Poland. *Nat. Phys. Sci.* **1973**, *241*, 16–17. [CrossRef]
24. Majorowicz, J. Heat flow map of Poland on the background of geothermal field of Europe and some aspects of its interpretation. *Acta Geophys. Pol.* **1976**, *24*, 147–156.
25. Wessel, P.; Smith, W.H.F. Free software helps map and display data. *Eos* **1991**, *72*, 441. [CrossRef]
26. Majorowicz, J.; Šafanda, J. Lithosphere Thickness from New Heat-Flow Data of the Odra Variscan Area, S-W Poland. *Pure Appl. Geophys.* **2018**, *175*, 4343–4354. [CrossRef]
27. Królikowski, C. Crustal-scale complexity of the contact zone between the Palaeozoic Platform and the East European Craton in the NW Poland. *Geol. Q.* **2006**, *50*, 33–42.
28. Karnkowski, P.H. Petroleum Provinces in Poland. *Prz. Geol.* **2007**, *55*, 1061–1067, (In Polish with English abstract).
29. Jessop, A.M.; Habart, M.A.; Sclater, J.G. The world heat flow data collection 1975. *Geotherm. Serv. Can. Geotherm. Ser.* **1976**, *50*, 55–77.
30. Vieira, F.; Hamza, V. Global Heat Flow: New Estimates Using Digital Maps and GIS Techniques. *Int. J. Terr. Heat Flow Appl. Geotherm.* **2018**, *1*, 6–13.
31. Kim, Y.; Huh, M.; Lee, E. Numerical Modelling to Evaluate Sedimentation Effects on Heat Flow and Subsidence during Continental Rifting. *Geosciences* **2020**, *10*, 451. [CrossRef]
32. MacKenzie, J.M.; Canil, D. Composition and thermal evolution of cratonic mantle beneath the central Archean Slave Province, NWT, Canada. *Contrib. Miner. Pet.* **1999**, *134*, 313–324. [CrossRef]
33. Heckenbach, E.; Norden, B.; Fuchs, S. Evaluation of the glacial impact on the shallow heat-flow density in the North German Basin. *Geophys. Res. Abstr.* **2019**, *21*. Available online: https://meetingorganizer.copernicus.org/EGU2019/EGU2019-12927-1.pdf (accessed on 7 September 2021).
34. Cermak, V. Lithospheric thermal regimes in Europe. *Phys. Earth Planet. Inter.* **1993**, *79*, 179–193. [CrossRef]
35. Cermak, V.; Safanda, J.; Guterch, A. Deep temperature distribution along three profiles crossing the Teisseyre-Tornquist tectonic zone in Poland. *Tectonophysics* **1989**, *164*, 151–163. [CrossRef]
36. Hasterok, D.; Chapman, D. Heat production and geotherms for the continental lithosphere. *Earth Planet. Sci. Lett.* **2011**, *307*, 59–70. [CrossRef]
37. Pollack, H.N.; Chapman, D.S. Mantle heat flow. *Earth Planet. Sci. Lett.* **1977**, *34*, 174–184. [CrossRef]
38. Narkiewicz, M.; Grad, M.; Guterch, A.; Janik, T. Crustal seismic velocity structure of southern Poland: Preserved memory of a pre-Devonian terrane accretion at the East European Platform margin. *Geol. Mag.* **2010**, *148*, 191–210. [CrossRef]
39. Artemieva, I.M. *The Lithosphere: An Interdisciplinary Approach*; Cambridge University Press: New York, NY, USA, 2011; p. 794. ISBN 9780521843966.
40. Correia, A.; Šafanda, J. Geothermal modeling along a two-dimensional crustal profile in Southern Portugal. *J. Geodyn.* **2002**, *34*, 47–61. [CrossRef]
41. Eppelbaum, L.V.; Kutasov, I.M.; Pilchin, A.N. *Applied Geothermics*; Springer: Berlin/Heidelberg, Germany, 2014.
42. Jaupart, C.; Mareschal, J.-C. Constraints on crustal heat production from heat flow data. In *Treatise on Geochemistry: The Crust*; Rudnick, R., Ed.; Elsevier: Amsterdam, The Netherlands, 2003; Volume 3, pp. 65–84.
43. Čermak, V.; Rybach, L. (Eds.) *Terrestrial Heat Flow in Europe*; Springer: Berlin/Heidelberg, Germany; New York, NY, USA, 1979; p. 328.
44. Čermak, V.; Hurtig, E. Heat flow map of Europe, 1:5,000,000. In *Terrestrial Heat Flow in Europe*; Čermak, V., Rybach, L., Eds.; Springer: Berlin/Heidelberg, Germany; New York, NY, USA, 1979.
45. Cloetingh, S.; van Wees, J.; Ziegler, P.; Lenkey, L.; Beekman, F.; Tesauro, M.; Förster, A.; Norden, B.; Kaban, M.; Hardebol, N. Lithosphere tectonics and thermo-mechanical properties: An integrated modelling approach for Enhanced Geothermal Systems exploration in Europe. *Earth Sci. Rev.* **2010**, *102*, 159–206. [CrossRef]

46. Hurtig, E.; Čermak, V.; Haenel, R.; Zui, V.I. *Geothermal atlas of Europe*; Hermann Hack Verlagsgesellschaft: Geographisch-Kartographische Anstalt: Gotha, Germany, 1992.
47. Guterch, A.; Wybraniec, S.; Grad, M.; Chadwick, R.A.; Krawczyk, C.M.; Ziegler, P.A.; Thybo, H.; De Vos, W. Crustal structure and structural framework. In *Petroleum Geological Atlas of the Southern Permian Basin Area*; Doornenbal, J.C., Stevenson, A.G., Eds.; EAGE Publications: Houten, The Netherlands, 2010; pp. 11–23.
48. Fuchs, S. The variability of rock thermal properties in sedimentary basins and the impact on temperature modelling—A Danish example. *Geothermics* **2018**, *76*, 1–14. [CrossRef]
49. Norden, B.; Förster, A.; Balling, N. Heat flow and lithospheric thermal regime in the Northeast German Basin. *Tectonophysics* **2008**, *460*, 215–229. [CrossRef]
50. Marks, L. Timing of the Late Vistulian (Weichselian) glacial phases in Poland. *Quat. Sci. Rev.* **2012**, *44*, 81–88. [CrossRef]
51. Wróblewska, M. Opracowanie modeli termicznych litosfery obszaru SE Polski. In *Kompleksowa Interpretacja Anomalii Pól Potencjalnych Wzdłuż Wszystkich Profili Głębokich Badań Refrakcyjnych Zrealizowanych na Całym Obszarze CELEBRATTION 2000. Arch*; Grad, M., Guterch, A., Eds.; Ministry of Environment: Warsaw, Poland, 2008.
52. Simmons, N.A.; Forte, A.; Boschi, L.; Grand, S.P. GyPSuM: A joint tomographic model of mantle density and seismic wave speeds. *J. Geophys. Res. Space Phys.* **2010**, *115*. [CrossRef]
53. Šimonová, B.; Zeyen, H.; Bielik, M. Continental lithospheric structure from the East European Craton to the Pannonian Basin based on integrated geophysical modelling. *Tectonophysics* **2018**, *750*, 289–300. [CrossRef]
54. Bellani, S. Update of Heat Flow Data in the Geothermal Areas of Tuscany, Italy. *GRC Trans.* **2018**, *42*, 861–870.
55. Szuman, I.; Kalita, J.Z.; Ewertowski, M.W. The impact of geothermal heat flux on the last Scandinavian ice sheet over W Poland and E Germany. *Geogr. Ann. Ser. A Phys. Geogr.* **2018**, *100*, 388–403. [CrossRef]
56. Chapman, D.S.; Furlong, K.P. Thermal state of the continental lower crust. In *Continental Lower Crust*; Fountain, D.M., Arculus, R., Kay, R.W., Eds.; Elsevier: Amsterdam, The Netherlands, 1992; pp. 179–199.
57. Lüthgens, C.; Böse, M. Chronology of Weichselian main ice marginal positions in north-eastern Germany. *E G Quat. Sci. J.* **2011**, *60*, 236–247. [CrossRef]
58. Schlosser, P. Einbeziechung petrophysikalisher bohr-lochmesergebnisse in bestimmungen des terrestrischen warmeflusses. *Geophys. Geol* **1970**, *15*, 13–32.
59. Agemar, T.; Weber, J.; Schulz, R. Deep Geothermal Energy Production in Germany. *Energies* **2014**, *7*, 4397–4416. [CrossRef]
60. Barker, C. Thermal Modeling of Petroleum Generation: Theory and Applications. In *Developments in Petroleum Science 45*; Elsevier: Amsterdam, The Netherlands, 1976; p. 512.
61. Griffiths, C.M.; Brereton, N.R.; Beausillon, R.; Castillo, D. Thermal conductivity prediction from petrophysical data: A case study. *Geol. Soc. London, Spéc. Publ.* **1992**, *65*, 299–315. [CrossRef]
62. Blackwell, D.D.; Steele, J.L. Thermal conductivity of sedimentary rocks: Measurement and significance. In *Thermal History of Sedimentary Basins, Methods and Case Histories*; Naeser, N.D., McCulloh, T.M., Eds.; Springer: Berlin/Heidelberg, Germany; New York, NY, USA, 1989.
63. Blackwell, D.D.; Richards, M. (Eds.) *Heat Flow Map of North America*, 1st ed.; AAPG: Tulsa, OK, USA, 2004; ISBN 0791815722.
64. Blackwell, D.D.; Beardsmore, G.R.; Nishimori, R.K.; McMullen, R.J. High-Resolution Temperature Logs in a Petroleum Setting: Examples and Applications. *Geotherm. Basin Anal.* **1999**, 1–34. [CrossRef]
65. Wilde-Piórko, M.; Świeczak, M.; Grad, M.; Majdański, M. Integrated seismic model of the crust and upper mantle of the Trans-European Suture zone between the Precambrian craton and Phanerozoic terranes in Central Europe. *Tectonophysics* **2010**, *481*, 108–115. [CrossRef]